CAUSTIC STRESS CORROSION CRACKING IN IRON-CHROMIUM-NICKEL AUSTENITIC ALLOYS

C. Barillec, M. Bonningue, D. Hocquellet, J.Y. Boos

Départ. Métal., Ecole Nationale Supérieure des Mines
158 Cours Fauriel, 42023 Saint-Etienne Cédex, France

ABSTRACT

Specimens of Fe-Cr-Ni alloys have been submitted to tensile tests, performed in a 750 g/l NaOH solution, at a temperature of 350°C and under a pressure of 100 bar. For each test, the strain rate was fixed at a given value, in the range of 10^{-6} to $10^{-2}s^{-1}$. On the value of this rate depend, on one hand, the mechanical characteristics of ductility and strength of the metal, and, on the other hand, the morphological aspects of cracks and fracture surfaces.

KEYWORDS

Stress corrosion cracking, iron-chromium-nickel austenitic alloys, tensile tests, sodium hydroxide, trace elements, single crystals.

INTRODUCTION

Fe-Cr-Ni austenitic alloys are widely used in the construction of electro-nuclear power plants. They are not, however, totally free from the risk of stress corrosion cracking (SCC), in particular when a heavily alkaline environment builds up; this can occur, for example, in the PWR Steam generators.

SCC takes place in a material which is submitted simultaneously to the action of mechanical stresses, applied or residual, and of a corrosive environment, to which it is, normally, fairly chemically resistant. Thus, the SCC of a metal results, a priori, from a competition between four basic mechanisms :

- microscopic plastic deformation
- dissolution in an active state
- dissolution in a passive state
- repassivation

By mastering the kinetics of each of them, we should master their synergistic effects. Among the three categories of SCC tests :

- constant strain tests
- constant load tests
- constant strain rate tests

it is thus the last category which is the most suitable to the elucidation of the phenomenon. With the goal of applying this type of test to the study of caustic SCC

in Fe-Cr-Ni alloys, we have designed and built a novel apparatus (Buscarlet and co-workers, 1980). It is an autoclave, in which one can carry out tensile tests at the heart of a concentrated hydroxide solution, at a prescribed temperature and under pressure.

When studying a corrosion phenomenon, it is often necessary to take not only the nominal composition of the alloy into account, but also the trace elements it contains. Various authors have demonstrated that certain trace elements, namely C, S, P, N, can influence the SCC resistance of INCONEL 600 in pure water (Coriou and co-workers, 1969; Domian and co-workers, 1976), in acid environments (Vermilyea and co-workers, 1975), and in alkaline environments (McIlree and co-workers, 1975,1977; Pessall and co-workers, 1979). In order to isolate the specific influence of each trace element, we have compared the behaviors of high purity and doped grades, elaborated from iron, chromium and nickel which were refined in our laboratory.

Another factor to be considered is the heat treatment of the alloy. Other authors (Berge and co-workers, 1977; Airey, 1979) have shown in effect the influence of a heat treatment of 16 h at 700°C on the SCC resistance of INCONEL 600.

EXPERIMENTS

Materials and Heat Treatments

Fifteen alloys were taken into consideration, two of which were available commercially, and thirteen of which were prepared in the laboratory. Their compositions are shown in the following table :

Designation	C	Fe	Cr	Ni	Mo	P	S
Commercial 304 L	0.0280	Bal	18.0	10.3		0.0200	0.0080
Commercial 316 L	0.0210	Bal	17.2	11.6	2.0	0.0140	0.0140
17-13	0.0054	Bal	16.8	12.6		< 0.0015	0.0050
17-13 HP	0.0048	Bal	16.8	12.6		< 0.0015	0.0025
17-13 HP-S	0.0030	Bal	16.1	12.7		< 0.0015	0.0320
17-13 UHP	0.0017	Bal	16.6	13.1		< 0.0015	< 0.0010
Alloy 800	0.0050	Bal	18.5	30.6		< 0.0030	0.0050
18-54	0.0033	31.5	18.4	Bal		< 0.0030	0.0070
Synthetic alloy 600	0.0060	9.9	14.3	Bal		< 0.0015	0.0025
Alloy 600 HP	0.0024	8.2	18.5	Bal		< 0.0015	0.0020
Alloy 600 UHP	0.0020	8.6	17.7	Bal		< 0.0015	< 0.0010
Alloy 600 UHP-C	0.0120	8.2	18.5	Bal		< 0.0015	0.0020
Alloy 600 UHP-S	0.0020	8.1	17.8	Bal		< 0.0015	0.0230
36-33	0.0080	Bal	34.8	31.9		< 0.0030	0.0080
36-54	0.0070	12.3	36.1	Bal		< 0.0030	0.0070

From each of these alloys about twenty cylindrical tension test specimens were taken. Their calibrated section has a cross sectional area S_o = 6 mm^2 and a length l_o = 12 mm.

Their ends are cone shaped.

All of the samples were water quenched after annealing for 1 h between 1050 and 1200°C. Some of them were, in addition, heat-treated by ageing for 16 h at 700°C.

Tensile Tests. Layout of the Rational Curves

The samples were submitted to tensile tests at 350°C :
- on the one hand in air, considered here as the reference environment
- on the other hand in a 750 g/l NaOH solution, under 100 bar of pressure.

The range of strain rates explored goes from 10^{-2} to 10^{2} µm.s^{-1}. For our samples that corresponds to relative elongation rates of 10^{-6} to 10^{-2} s^{-1}.

Each test directly supplies two mechanical characteristics : the tensile stress R and the elongation to fracture A. Measuring the reduction of area is difficult because of the small size of the samples.

But the data supplied by a tensile test are not limited to the quantities A and R. The behavior of the material can be specified by the layout of the rational curve, which is deduced from the stress-strain experimental curve $F = f(\Delta l)$, by plotting the flow-stress :

$$\sigma = \frac{F}{S_o}\left(1 + \frac{\Delta l}{l_o}\right)$$

versus the rational elongation :

$$\varepsilon = \mathrm{Ln}\left(1 + \frac{\Delta l}{l_o}\right)$$

The performances of our tensile testing device permit us to use only the results relative to the plastic behavior of the material.

Fractographic Observations

After the tensile test, each sample is submitted to two fractographic examinations. The first, which is done by scanning electron microscope (SEM), is used to observe the fracture surface which may present three classic features :
- Dimples, typical of transgranular ductile fracture (D)
- Transcrystalline quasicleavages with river patterns, typical of transgranular brittle fracture in metals with fcc crystal structures (T).
- "Rock candy" intergranular fracture, typical of grain boundary decohesion (I).

The second examination, which is done with an optical microscope on a polished longitudinal section is used to study the cracks which may have formed in the metal before fracture.

RESULTS

Influence of the Strain Rate on the Behavior of Alloy 800

The behavior of the water quenched Alloy 800 is rather representative of the whole of the set of alloys considered.

In terms of the strain rate $\dot{e}$, in air or in NaOH, the elongation to fracture A (Fig. 1) and the tensile stress R vary in the same way. In air, the A and R characteristics vary only slightly in relation to the strain rate. In NaOH, on the contrary, it appears a range of rates in which R and especially A vary considerably.

At a high strain rate, the A and R values are about the same in air or in NaOH. Below a strain rate V_1, the A and R values are lower in NaOH than in air : this rate characterizes the appearance of the SCC phenomenon. The elongation to fracture A tends to become independent of the strain rate when the latter falls below a value V_2. On the whole, this behavior is similar to that of stainless steels in a chloride environment (Desestret and others, 1977).

Examination of the fracture surfaces by SEM reveals important morphological differences. Samples air broken, at all strain rates, exhibit a transgranular ductile fracture with dimples (D), which, furthermore, is accompanied by necking. The same is true for samples broken in NaOH, at a rate greater than V_1. At a lower rate, the fracture surfaces exhibit two features : transgranular quasicleavages (T) in an external ring, dimples (D) in the center. This core with dimples retracts as the rate is decreased, and practically disappears at rates lower than V_2. At these rates, local areas of intergranular fracture (I) can appear, but will not be widespread. This observation suggests that the cracking can initiate intergranularly and then propagate transgranularly. From the whole of these fractographic observations, what stands out is that the appearance of the SCC coincides with that of a fracture which is not entirely ductile.

The rational tensile curve of Alloy 800 , in air at 350°C, is practically independent of the strain rate. It sets off the three standard stages of the deformation of the fcc metals. In NaOH, the two first stages appear entirely at all strain rates. On the other hand, the third stage, which is complete at high rates, progressively disappears as the rate decreases, between V_1 and V_2. Furthermore, it has been verified that the A and R values are always greater than the coordinates ε_{23} and σ_{23} of the connecting point of stages 2 and 3. Hence, it appears that these are the plastic deformation mechanisms of stage 3 that come into play in the SCC phenomenon. This is confirmed by the following observation : a test at a very low rate, interrupted in stage 2, causes no cracks to appear in the sample.

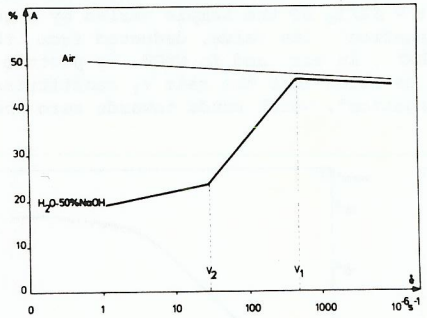

Fig. 1 - Effect of strain rate on the elongation to fracture of the Alloy 800 in two environments at 350°C.

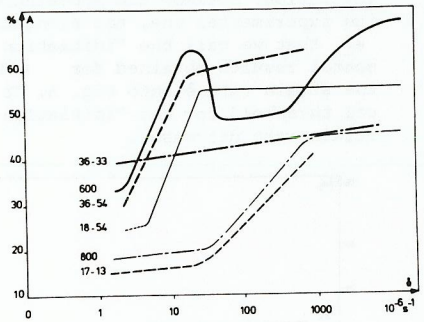

Fig. 2 - Effect of strain rate on the elongation to fracture of various Fe-Cr-Ni alloys in a 750 g/l NaOH solution at 350°C.

Behavior of Alloys Containing Various Proportions of Iron, Chromium and Nickel

In air at 350°C, the various water quenched Fe-Cr-Ni alloys exhibit, like Alloy 800 , mechanical characteristics which vary only slightly in relation to the strain rate. The results of the tensile tests done on the same alloys in NaOH (Fig. 2), set off the following differences with Alloy 800 :

→ The 17-13 stainless steel exhibits more intergranular fractures.

→ For the 18-54 and 36-54 alloys the critical rate V_1 is around 100 times less than for . They would thus be less susceptible to SCC. On the other hand, below the strain rate V_1, the decrease of their elongation to fracture is more abrupt.

→ The 36-33 alloy does not exhibit a critical rate in the range of rates studied, and would thus be the most resistant to SCC.

→ Finally, Alloy 600 behaves like the 54 % Ni alloys at low rates, but exhibits another drop in ductility when in the range of the high strain rates.

Influence of Trace Elements and of Heat Treatment on the Behavior of the Alloy 600

In air at 350°C, all the grades of the water quenched Alloy 600 exhibit the same behavior, namely an elongation to fracture on the order of 70 %, regardless of the strain rate. Only in the case of the ultra high purity sulphur doped grade (UHP-S) is the elongation smaller. The heat treatment does not influence the extent of elongation, except for the high purity grade (HP), in which case it decreases the elongation to the level of that of the sulphur doped grade (UHP-S).

In NaOH at 350°C, after water quench, the carbon doped grade (UHP-C) is the most resistant to SCC, and the sulphur doped grade (UHP-S) is the least resistant (Fig. 3). Curiously, three grades of the water quenched Alloy 600 exhibit a drop in ductility, in a range of strain rates greater than V_1 : this concerns the grades referred to as "synthetic", "HP" and "UHP-C". For the last two, the drop in ductility is shifted towards the higher rates. The drop in ductility is observed neither for the ultra high purity grade (UHP), nor for the sulphur doped grade (UHP-S). nor for any grade after sensitizing heat treatment. This treatment also influences the critical strain rate V_1, in other words, the SCC appearance threshold (Fig. 3). This treatment has a positive effect on the synthetic grade, on the "HP" and "UHP-S" grades. On the contrary it has a negative effect on the "UHP" and "UHP-C" grades.

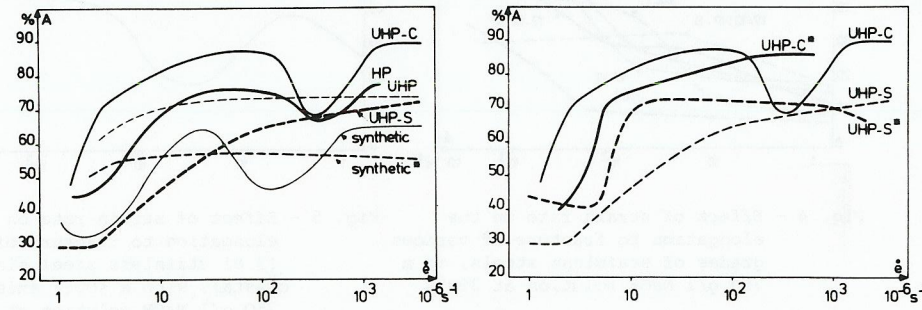

Fig. 3 - Effect of strain rate on the elongation to fracture of various grades of Alloy 600 , in a 750 g/l NaOH solution at 350°C (*after ageing for 16 h at 700°C).

The grade composition and the heat treatment, as well as the elongation rate, influence the fracture mechanism of the samples deformed in NaOH. As the strain rate increases from 10^{-6} to 10^{-2} s^{-1}, the following features are successively observed :
→ I, I + D, D, for the "synthetic", the "UHP-S" and the sensitized "UHP-C" grades.
→ I, T + D, D, for the "HP" grade and the water quenched "UHP-C" grade.
→ T, D, for the "UHP" grade.
In the ductility drop, the water quenched synthetic grade exhibits an intergranular

fracture (I).

Influence of the Trace Elements on the Behavior of Stainless Steel

In air at 350°C, all of the water quenched 17-13 steel grades exhibit an elongation to fracture on the order of 60 %, regardless of the strain rate. Necking on the samples is considerable. The fracture surfaces all exhibit dimples.

In NaOH at the same temperature (Fig. 4), the 17-13 steel grades elaborated in the laboratory, of ordinary purity, high purity or ultra high purity, behave virtually in the same manner. For the commercial grade 304 L, the critical rate V_1 is lower than for the previous grades; but if the SCC range appears to be more limited, the decrease in mechanical properties involved is relatively more important. On the contrary, the commercial grade 316 L with molybdenum exhibits high SCC sensitivity, since within the explored range of rates it does not entirely recover the properties it has in air. The influence of a sulphur addition is not clear : the tensile stress R remains low in the entire rate range studied, whereas at low rates the elongation to fracture A is higher than for the sulphur poor grades.

In NaOH, the fracture of the two commercial grades 304 L and 316 L evolve in the same way as that of Alloy 800 : as the strain rate increases, onecan observe successively transgranular quasicleavages and then dimples. The increase in purity of the steel makes itself known especially through the disappearance of the transgranular fracture mode, to the benefit of intergranular fractures, below the critical threshold V_1. The presence of sulphur in large quantities delays the appearance of the dimpled transgranular fractures, which are characteristic of a ductile metal.

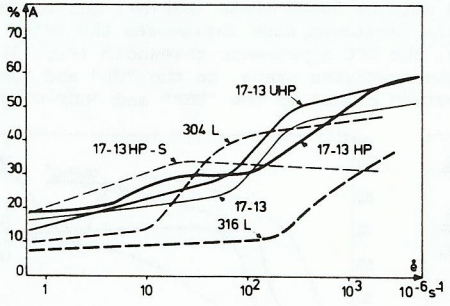

Fig. 4 - Effect of strain rate on the elongation to fracture of various grades of stainless steels, in a 750 g/l NaOH solution at 350°C

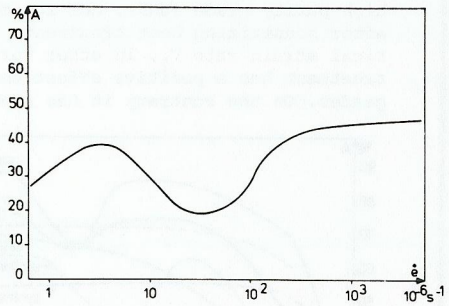

Fig. 5 - Effect of strain rate on the elongation to fracture of 17 Cr-13 Ni stainless steel single crystals with a <001> axis, in a 750 g/l NaOH solution at 350°C.

Behavior of Single Crystals of Austenitic 17 Cr - 13 Ni Steel

Stainless steel single crystals were prepared by controlled solidification. Their chemical composition is as follows :

C	Cr	Ni	P	S
0.01% - 0.03%	17.1% - 18.2%	12.7% - 14.0%	< 0.001%	< 0.001%

Tensile samples with a <001> axis were taken from them and machined by spark erosion; the sides of the sample, rectangular in section, are (100) planes.

In NaOH (Fig. 5), there is still a critical strain rate V_1 above which the mechanical properties are the same as in air. This rate corresponds to the one which characterizes the polycrystalline alloy. But, in addition, there is a lower critical rate, below which there is no more SCC : examination of cuts made in samples confirms this result, since it only reveals generalized corrosion.

Above the lower threshold, as the rate increases, the number of crack initiations multiplies, it seems from corrosion pits. The maximal deterioration field is characterized by the presence of wide cracks which cross the sample from one side to the other. Improvement of the mechanical properties with the increase of the tensile rate is accompanied by ramification of the cracks. At the highest rates, the cracks are very wide, as if opened by the deformation. The crystallographic character of the propagation of the cracks is visible on the micrographs of sample cuts.

DISCUSSION

Study of the Cracking of Alloy 800

The cracking of the metal in a corrosive environment can be broken down into two stages : initiation then propagation of the cracks. In accordance with the experimental observations, we consider that initiation has begun as soon as stage 3 appears on the rational tensile curve. As far as propagation is concerned, we consider that it comes into play at the top of the experimental curve, since the deformation become localized at that time. Detailed analysis of the cracked surface reveals that at the top of curve the useful part of the sample is only reduced by an average of around 2 %; hence a crack can propagate when its depth reaches around 13 µm.

Initiation. Between the appearance of stage 3 on the rational curve and the top of the experimental one, the elongation $e = \Delta l/l_o$ of the sample varies by a quantity e_i, that we call the "initiation elongation". Its value, deducted from the experimental results obtained for Alloy 800 , in air and in NaOH, is plotted versus the strain rate $\dot{e}$ onto Fig. 6. It can be noted that the rate V_1 constitutes a critical threshold for the "initiation elongation", which tends towards zero when the strain rate decreases.

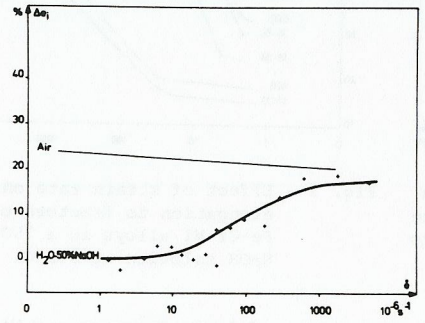

Fig. 6 - Effect of strain rate on the "initiation elongation" of Alloy 800 in air and in a 750 g/l NaOH solution at 350°C

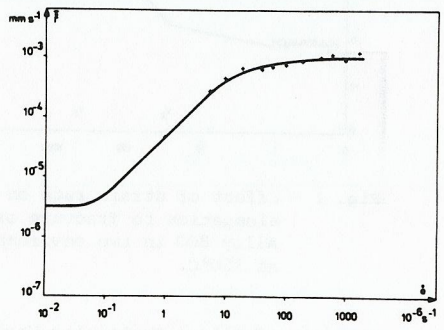

Fig. 7 - Effect of strain rate on the crack propagation rate in Alloy 800, in a 750 g/l NaOH solution at 350°C.

Propagation. Between the top of the tensile experimental curve and the fracture of the sample, its elongation $e = \Delta l / l_o$ varies by a quantity Δe_p, which we call the "propagation elongation". The propagation duration t_p of the cracks is the product of Δe_p by the strain rate $\dot{e}$ of the sample. If we take the hypothesis of a radial propagation of the cracks, their ultimate depth is equal to the width of the ring exhibiting transgranular quasicleavages with river patterns. The average propagation rate $\dot{r}_p$ of the cracks is thus written :

$$\dot{r}_p = \frac{r_p}{t_p} = \frac{r_p}{\dot{e} . \Delta e_p}$$

Its value, deducted from the experimental results obtained for the 800 alloy in sodium hydroxide, is plotted versus the strain rate $\dot{e}$ onto Fig. 7. It can be noted this time that it is the rate V_2 which becomes the critical threshold : above V_2, the average crack propagation rate $\bar{\dot{r}}_p$ is constant and equal to 10^{-3} mm/s; below V_2, it is proportional to the strain rate $\dot{e}$.

Interpretation of the Cracking

It is possible to reconstitute the curve of Fig. 7 from the metal deformation and corrosion kinetics, by writing that the deformation is discrete : on a given area of the surface, an event takes place at intervals of time Δt which strips the metal, the corrosion of which then takes place according to a current density $i(t)$. The event may be the formation of a constant height h slip step, or an intergranular slip. The average cracking rate is written $\bar{r}$:

$$\bar{r} = \frac{K}{\Delta t} \int_0^{\Delta t} i(t)\, dt \quad \text{with} \quad K = \frac{M}{nF}$$

M : atomic weight of the metal
n : number of electrons exchanged
: density of the metal

This is cracking by anodic dissolution.
The samples are at such a potential that their attack follows a prepassivation kinetics :

$$i = i_o [(1 - \chi) + \chi \exp(-\beta t)]$$

As demonstrated for nickel in an acid environment (Schwabe and Ebersbach, 1972), this expression differentiates itself from pure passivation kinetics by the term $\chi \neq 1$.
The time interval Δt depends on the strain rate $\dot{e}$; if we consider only the first term of a series expansion, we can write :

$$\Delta t = \frac{\alpha}{\dot{e}}$$

The average cracking rate thus becomes :

$$\bar{r} = K i_o (1 - \chi) + \frac{K i_o}{\alpha\beta} [1 - \exp(-\frac{\alpha\beta}{\dot{e}})] \dot{e}$$

Potentiostatic measurements have shown us that the term $i_o (1 - \chi)$ is about 10^{-2} A.cm^{-2}. We can then adjust $\bar{r}$ to the curve of the Fig. 7 by taking :

$$\chi = 1 - 10^{-3}$$
$$\alpha\beta = 2.02 . 10^{-5}$$
$$i_o = 2.7 \text{ A.cm}$$

Actually, two non-defined parameters remain : α and β. We will suppose for the remaining part that $\beta = 1$, which means that the "reprepassivation" is not very rapid (Hoar and Ford, 1973; Scully, 1978). As for the α parameter, we can understand its significance by writing the relationship between a slip γ and the overall elongation ε :

$$d\gamma = m_T\, d\varepsilon$$

The term m_T is the Taylor factor for the polycrystals, and is equal to 3.06 for an fcc metal. If the deformation is localized in a p width zone at the tip of the crack, h height slip steps are produced at Δt time intervals :

$$\frac{h}{p} = m_T \dot{e} \frac{l}{p} \Delta t \neq \Delta t = \frac{h}{l m_T} \neq \alpha = \frac{h}{l m_T}$$

Fr l = 10 mm and $\alpha = 2.02\ 10^{-5}$, we obtain h = 0,5 µm, which is a reasonable size, since it corresponds to dislocations emitted by groups of around 3000.

This model is similar to other ones, proposed for the interpretation of currents measured in rapid tensile tests in a corrosive environment, at an imposed potential (Murata and Staehle, 1974). Comparison of the mechanical and electrochemical kinetics shows that below V_2 it is the mechanical kinetics which imposes the SCC one, and that between V_2 and V_1 the kinetics is mixed, Above V_1, the deformation takes place according to another mechanism and again imposes its kinetics, but this no longer concerns SCC, whose appearance is thus characterized by the V_1 rate.

CONCLUSION

Tensile tests at an imposed strain rate, carried out in a corrosive environment, constitute a relatively new way of approaching problems of SCC.

Applied to Fe-Cr-Ni alloys in a 750 g/l NaOH solution, at 350°C, these tests bring out the existence of a critical strain rate, which is likely to characterize the resistance of the metal to SCC. In fact, below this rate, the material's mechanical properties are lower than in a non-aggressive environment, and its fracture is not entirely ductile. The layout of the tensile rational curve reveals that it is the mechanisms of stage 3 of the plastic deformation of the fcc metals which come into play in this phenomenon, in the case of Alloy 800 . For stainless steel single crystals, there is a second critical rate, below which there is no more SCC.

Examination of the behavior of various grades of austenitic Fe-Cr-Ni alloys, from 17 Cr - 13 Ni stainless steel, passing through Alloy 800 to Alloy 600 , demonstrates the role of the respective proportions of the three basic elements. Of all those which were studied, it is the Fe-36Cr-33Ni alloy which was the most resistant to SCC. Taking into consideration high purity grades, certain of which were carbon or sulphur doped, demonstrates that trace elements can influence the behavior of the alloys, as well as the heat treatments themselves.

The hypothesis of a discontinuous plastic deformation at the tip of the cracks, in other words of a stripping of the metal at regular time intervals, allows one to quantitavely interpret the main experimental results.

ACKNOWLEDGEMENT

The authors are grateful to Professor C. GOUX for encouragement to undertake this work.

REFERENCES

Airey, G.P. (1979). Corrosion, 35, 129-136
Berge, Ph., J.R. Donati, B. Prieux, and D. Villard (1977). Corrosion, 33, 425-435
Buscarlet, C., D. Hocquellet, C. Barillec, M. Bonningue and J.Y. Boos (1980) Corros. Sci., 20, 293-299
Coriou, H., L. Grall, P. Olivier and H. Willermoz (1969). Proceedings of conference Fundamental Aspects of Stress Corrosion Cracking, The Ohio State University (1967) NACE, Houston, pp. 352-359.
Desestret, A., F. Gauthey, J.L. Ranvier, J.C. Colson (1977). Mém. Sci. Rev. Mét., 74, 393-409
Domian, H., R.H. Emanuelson, L. Katz, L.W. Sarver, and G.J. Theus (1976). Babcock and Wilcox, Technical paper RDTPA 75-19
Hoar, T.P., and F.P. Ford (1973). J. Electrochem. Soc., 120, 1013-1019
McIlree, A.R., H.T. Michels and P.E. Morris (1975). Corrosion, 31, 441-448
McIlree, A.R., and H.T. Michels (1977). Corrosion, 33, 60-72
Murata, T., and R.W. Staehle (1974). Proceedings 5th International Congress on Metallic Corrosion, held in Tokyo (1972), NACE, Houston, pp. 513-518
Pessal, N., G.P. Airey and B.P. Lingenfelter (1979). Corrosion, 35, 100-107
Schwabe, K., and U. Ebersbach (1972). Proceedings 4th International Congress on Metallic Corrosion, held in Amsterdam (1969), NACE, Houston, pp. 709-713
Scully, J.C. (1978). Metal Science, 290-302
Vermilyea, D.A., C.S. Tedmon, Jr, and D.E. Broecker (1975). Corrosion, 31, 222-223